ILETA International Information and Engineering Technology Association

International Journal of Design & Nature and Ecodynamics

Vol. 20, No. 8, August, 2025, pp. 1837-1845

Journal homepage: http://iieta.org/journals/ijdne

Geochemical Characterization and Classification of Volcanic Materials from the Bromo-Tengger-Semeru Complex, East Java, Indonesia



Dwa Desa Warnana^{1*}, Siti Zulaikah², Amien Widodo¹, Wien Lestari¹, Juan Pandu Gya Nur Rochman¹, Sigit Tri Wicaksono³, Fadhilah⁴, Hanif Izzudin Zakly⁵, Aditya Pratama⁵, Nordiana Mohd Muztaza⁶, Rodeano Roslee⁷

- ¹ Department of Geophysical Engineering, Faculty of Civil Planning and Geo-Engineering, Institut Teknologi Sepuluh Nopember, Surabaya 60111, Indonesia
- ² Department of Physics, Faculty of Mathematics and Natural Science, Universitas Negeri Malang, Malang 65145, Indonesia
- ³ Department of Materials and Metallurgical Engineering, Faculty of Industrial Technology and Systems Engineering, Institut Teknologi Sepuluh Nopember, Surabaya 60111, Indonesia
- ⁴ Mining Department, Faculty of Engineering, Universitas Negeri Padang, Padang 25173, Indonesia
- ⁵ Research Center for Geological Disaster, National Research and Innovation Agency (BRIN), Bandung 40135, Indonesia
- ⁶ School of Physics, Universiti Sains Malaysia, Penang 11800, Malaysia
- ⁷ Faculty of Science and Technology, Universiti Malaysia Sabah, Kota Kinabalu 88400, Malaysia

Corresponding Author Email: dwa desa@geofisika.its.ac.id

Copyright: ©2025 The authors. This article is published by IIETA and is licensed under the CC BY 4.0 license (http://creativecommons.org/licenses/by/4.0/).

https://doi.org/10.18280/ijdne.200814

Received: 11 February 2025 Revised: 11 August 2025 Accepted: 15 August 2025

Available online: 31 August 2025

Keywords:

ultramafic lamprophyre aillikites, alkaline series absarokite, rare earth elements (REEs), Geochemical, Bromo-Tengger-Semeru volcanic material, XRF

ABSTRACT

Geochemical characterization has been widely carried out to classify the types of rocks and volcanic materials. Volcanic rocks are a major component of the Earth's crust and have their own unique characteristics. Classification and mapping are particularly beneficial for the exploration of specific minerals. This research focuses on studying and analyzing the geochemistry of volcanic materials in the Bromo-Tengger-Semeru (BTS) area, East Java, Indonesia. Whole-material geochemistry from 55 volcanic product samples from the BTS area was determined by X-ray fluorescence (XRF). The XRF results showed that the dominant compounds were CaO (12.5 Wt%), Fe₂O₃ (27.5 Wt%), and SiO₂ (41.3 Wt%). Results also reveal that mostly the BTS volcanic material was classified in the ultramafic lamprophyre Aillikites series. Meanwhile, the analysis based on the comparison of % K₂O vs. % SiO₂ values shows that BTS volcanic material is included in the alkaline series absarokite and belongs mainly to the post-caldera stage. These features potentially host rare earth elements (REEs)-bearing minerals.

1. INTRODUCTION

Geochemical analysis in several studies has classified the types of volcanic rocks [1-4]. This classification is useful for uncovering the origin of rocks and can even explain the recording of climate change that has occurred in the past [5, 6]. Furthermore, various research fields and applications in the field of volcanology employ geochemical analysis [7, 8]. Classification based on geochemical data has a role that can be used as a proxy indicator for the discovery of critical minerals or important minerals for the industrial world that can be mapped out for further exploration [9-12].

The volcanic material in each location has its characteristics [13, 14]. Mapping and classifying volcanic materials will be very useful to facilitate further exploration of specific minerals [1, 8]. Volcanic material in the form of igneous rocks usually has an abundant content of critical minerals or rare earth elements (REEs), and several previous studies have confirmed this [15-17].

The Bromo-Tengger-Semeru (BTS) in the Eastern part of the Java island, Indonesia, is one of the most visited basaltic andesitic volcanoes in the world [18], and is an ancient volcanic area that is still active [19-21]. The volcanic activity that occurs causes the rock formations in the BTS area to consist of young Quaternary rock formations to old Quaternary rock formations [22]. With such characteristics of volcanic activity and supported by existing rock formations, the BTS area should have the potential mineral abundance stored that can be mapped. However, several geochemical characterization studies have been limited to the active Mount Bromo area with its eruption products [23] and Tengger Caldera [24]. Studies on Mount Semeru are also limited to rock types based on potassium content [25] and focus more on studying disasters resulting from eruptions of Mount Semeru [26-28].

In this paper, we propose an investigation into the chemical content of BTS by X-ray fluorescence (XRF). The use of XRF has been tested effectively and efficiently, widely used to track the presence of minerals [23, 24, 29-32]. Firstly, we conducted a mapping of chemical compounds from volcanic materials, especially dominant compounds based on XRF data. Secondly, we analyse the characteristics of volcanic rocks based on their

SiO₂ and K₂O content [33] and the Si vs. Fe ratio [34]. The results of this analysis are expected to determine the classification of volcanic rock types at the study site. Thirdly, we emphasize the tectonic setting and volcanic environment on the formation of volcanic rocks in the BTS area by using Ti vs V plots [35] and ternary diagrams based on the comparison of the main elements MnO-TiO₂-P₂O₅ [36]. Finally, this study aims to characterize volcanic materials from the BTS area using XRF and classify them based on major element geochemistry to infer their origin and mineralization potential.

2. MATERIAL AND METHOD

2.1 Geology of Bromo-Tengger-Semeru

The Bromo-Tengger-Semeru (BTS) volcanic massif comprises a cluster of calderas and stratocones developed over a deeply eroded Tertiary volcanic arc in South Java [27]. The volcanic arc formed as a consequence of northward subduction along the Java Trench to the south with a convergence rate of about 7 cm per year (see Figure 1). Van Gerven and Pichler [24] explained that the oceanic plate subducts beneath the arc with a dip of $+65^{\circ}$, with the trench reaching a maximum depth of 6000-7000 m. The magmatic belt is superimposed upon old basement rocks, and the late Cenozoic volcanoes are built

mostly above Neogene marine strata [24].

The Bromo-Tengger caldera, with a diameter of about 8 km, formed during the Late Pleistocene (>45 ka and ca. 33 ka); resurgent volcanism has constructed four stratocones, including the active Bromo tuff cone [37]. Bromo volcano is located at 7°56.30'S and 112°57'E in geographical coordinates with an elevation of about 2329 meters above mean sea level (msl). Historically, Bromo volcano has erupted more than 50 times since 1775, and currently, it is the only active cone in Tengger caldera [23].

Mt. Semeru (8°06′05″S, 112°55′E), one of the most active volcanoes on Earth, is the highest mountain in Java (3,676 m) located 25 km to the south of Bromo (Figure 1) [24, 27]. Semeru's persistent and combined eruptive activity, at least since 1884, is unusual for calc–alkaline composite cones [27]. Semeru is superimposed on and buttressed to the north by the Jambangan complex. To the south and south-east, Semeru overlies weathered tuffs and breccias, and lava flows of the Oligocene–Miocene 'Tuf and Old Andesite formation [27].

The geological map of Bromo-Tengger-Semeru (BTS) can be seen in Figure 1. Based on geological information, the BTS consists of some sedimentary formations; they are: Tengger Volcanic Rock Formations (Qvt), Bromo Volcanic Rocks (Qvb), Tengger Volcanic Sand Formations (Qvs), and Avalanche Deposits from Nuee Ardente (Qvj) [38-41].

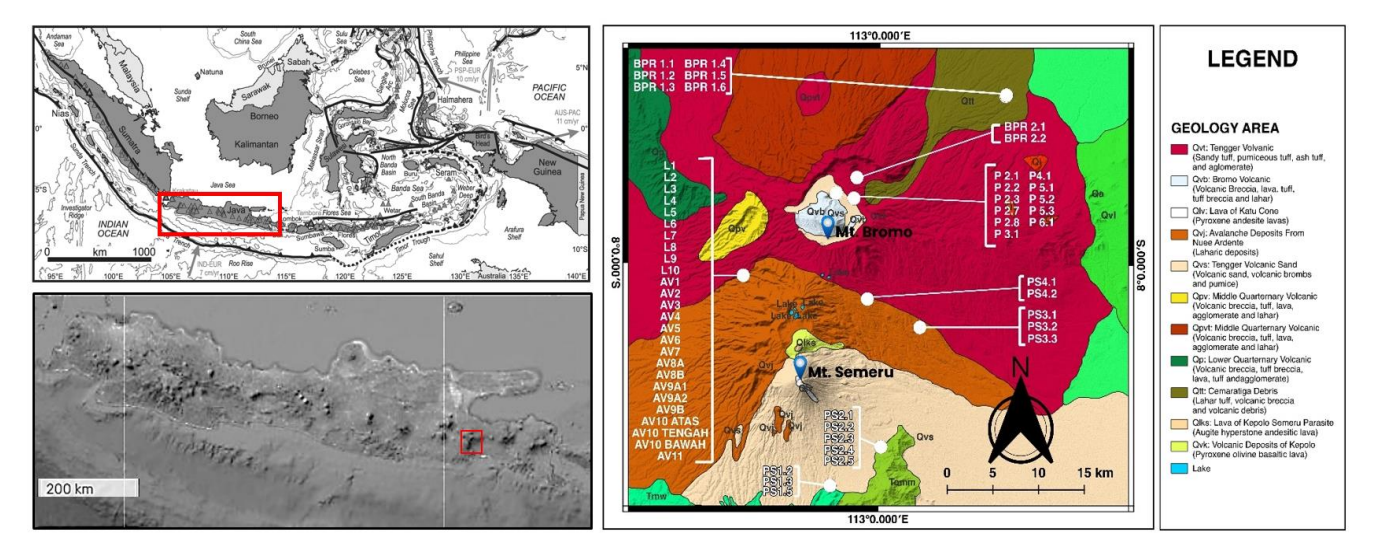


Figure 1. Sketch maps showing the regional tectonic setting of Indonesia, the island of Java, and the geological map of Bromo-Tengger-Semeru (BTS)

The white circle represents the sampling location.

2.2 Sampling and preparation

The samples were obtained from different locations in the Bromo-Tengger-Semeru (BTS) area. In addition to different locations, the samples in this study have various types of samples, including volcanic sand, gravel, volcanic ash, sandy soil, and andesite igneous rock. The difference in sample types is due to different geological formations (see Figure 1). Samples from the Bromo caldera area and the Semeru area are in the form of volcanic sand, sandy soil, and sandstone. Sampling was carried out on the surface at each sampling point. While samples in the form of andesite igneous rock from the Semeru area were sampled by looking at rock outcrops, which were then taken from the surface. Other samples from the Coban Pelangi area, in the form of gravel and volcanic ash, were obtained from outcrops in the form of walls located at the entrance to the Coban Pelangi tourist attraction, with a height

of 3 meters. Sampling at this location was carried out on the surface of the walls in each of its layers. A total of 55 samples were taken (see Appendix Table A1). From all the samples obtained, each sample was put into a standing pouch with an amount of \pm 1 kg.

Samples were obtained from outcrops that are suspected to be strong as a result of volcanic activity or the former eruption of Mount Bromo-Tengger-Semeru. Therefore, X-ray fluorescence (XRF) tests were performed in order to determine the chemical composition of the volcanic samples. Prior to XRF analysis, the samples were first dried and then smoothed until they became fine granules to eliminate physical effects such as particle size differences and reduce matrix effects. The detection limits for the major elements analyzed by XRF were approximately 0.01% [42].

To ensure data accuracy, standards were run alongside the samples during XRF analysis. Data quality was validated

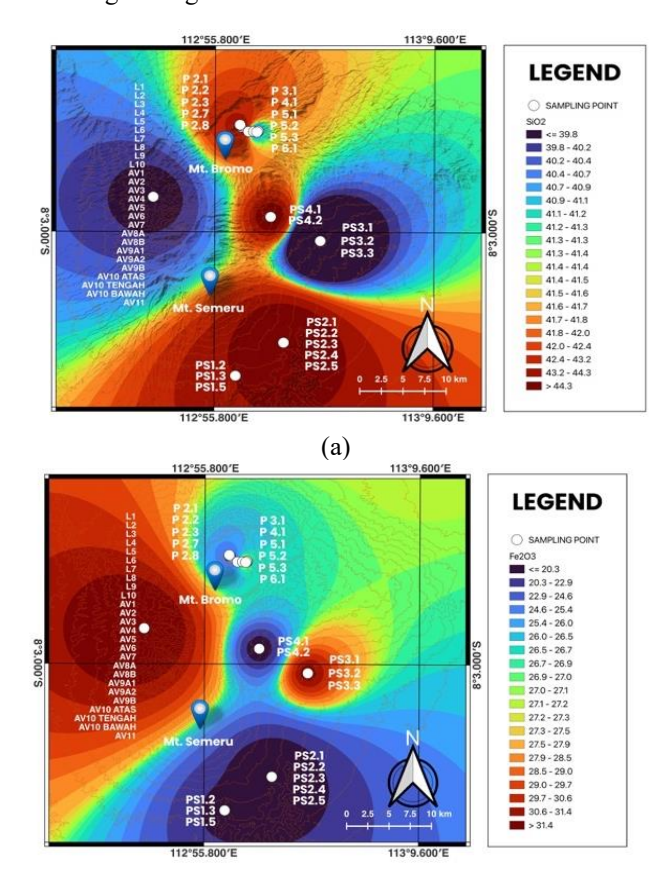
through repeated measurements of international reference materials, with accuracy maintained within \pm 5%. Furthermore, the geochemical data obtained were analyzed to classify the type and origin of volcanic material in the BTS area.

3. RESULTS AND DISCUSSION

3.1 Geochemical analysis

In general, the major element oxides measured from the BTS volcanic material sample consisted of Al₂O₃, SiO₂, K₂O, CaO, TiO₂, V₂O₅, Cr₂O₃, MnO, Fe₂O₃, CuO, SrO, BaO, Eu₂O₃, Re₂O₇, ZnO, P₂O₅, and Rb₂O (see Table 1). Based on the measured oxide compounds, there are dominant compounds from the BTS volcanic rock sample (>10 Wt%), including CaO (average 12.5 Wt%), Fe₂O₃ (average 27.5 Wt%), and SiO₂ (average 41.3 Wt%).

The results obtained from this geochemical test were then mapped with an interpolation technique to determine the distribution of dominant compounds (SiO₂, Fe₂O₃, and CaO) in the BTS area. Figure 2 shows the distribution of the three dominant compounds in the BTS area. Figure 2(a) shows that SiO₂ compounds are present in almost all samples of BTS's volcanic material. Spreads with high content are indicated in red. Fe₂O₃ compounds with the most dominant distribution are located in the Coban Pelangi at the AV10B point (see Figure 2(b)). Figure 2(c) shows the dominant distribution of CaO at four sampling points in the Mount Semeru area. The sampling points are PS 1.1, PS 1.2, PS 1.3, PS 1.5, PS 2.1, PS 2.2, PS 2.3, PS 2.4, PS 3.1, PS 3.2, PS 3.3, PS 4.1, PS 4.2. The range of CaO content in this region is between 13.7-19 wt%, with PS 2.4 having the highest CaO content.



(b)

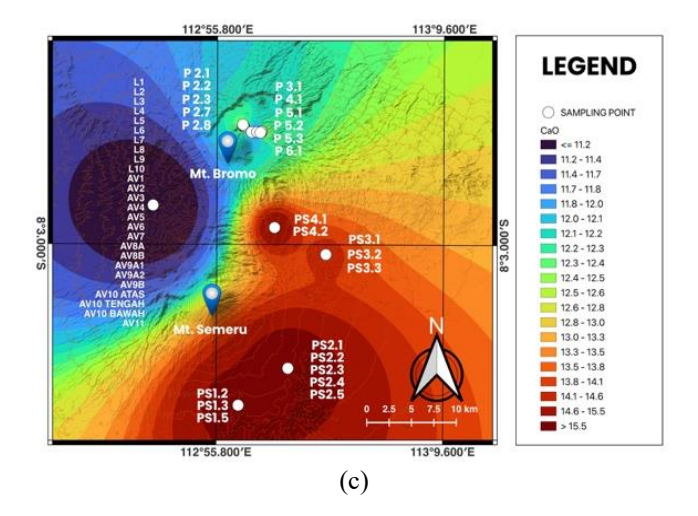


Figure 2. Map of the distribution of dominant compounds in the BTS area (a) SiO₂; (b) Fe₂O₃; (c) CaO

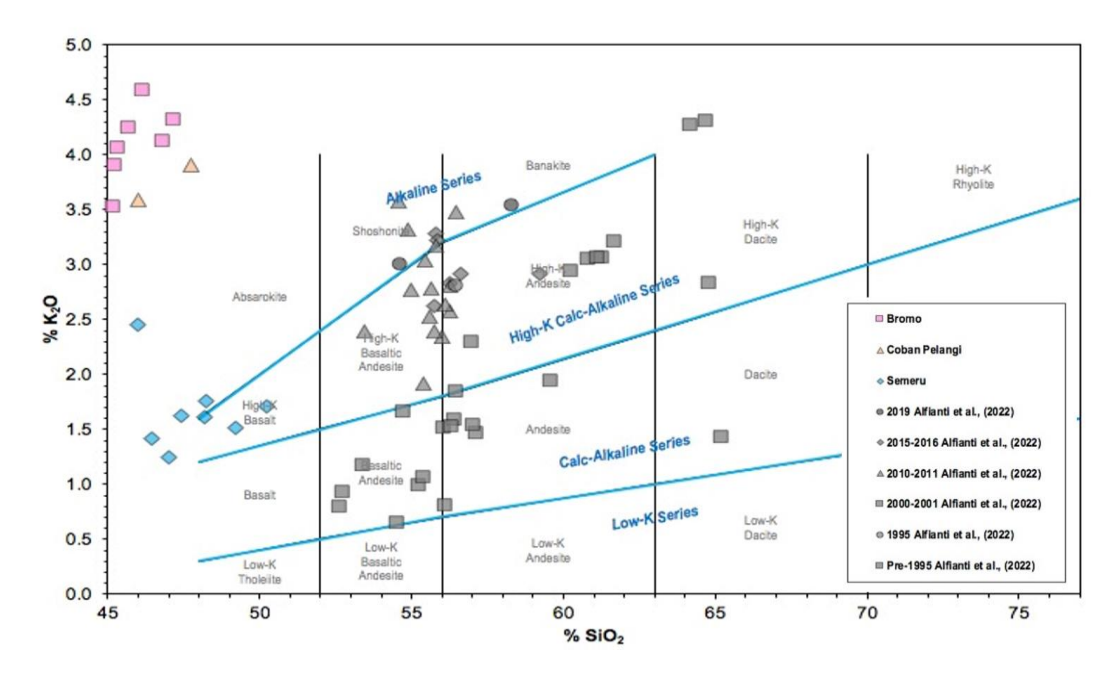
The Fe_2O_3 content in Bromo-Semeru is a larger amount than that in Arjuno-Welirang. However, the Fe-oxides measured in Arjuno-Welirang are only in samples of volcanic igneous rocks. This result may be because the structure of the BTS rock formation has different chemical content [43]. Furthermore, the dominance of Fe_2O_3 and differences in CaO and SiO_2 distribution in the BTS area reflect changes in magmatic processes or magmatic evolution as a product of volcanic activity in the research area. These results are in accordance with several studies, which show that the composition of Fe, CaO, and SiO_2 can reflect the evolution of magmatic processes [44-46].

3.2 Classification of volcanic materials

Rock classification was performed to study the characteristics of rocks from samples obtained from the field based on the results of geochemical tests. Classification is carried out to determine the type and origin of volcanic samples obtained from the field. Generally, volcanic samples from the BTS area were obtained from three different locations and geological formations.

Classification to determine the type of volcanic sample is done by comparing the SiO₂ and K₂O content from the results of geochemical tests [33] (Figure 3). The classification of volcanic rocks given by Peccerillo and Taylor [33] has been useful and widely accepted. Based on Figure 3, volcanic samples originating from the Bromo-sand sea caldera are generally classified as alkaline series absarokite. Meanwhile, most samples from the Semeru area were classified in the high-K basalt type, some of which were classified in the alkaline series of the absarokite series. Samples taken from the Coban Pelangi site are almost all undefined due to their low SiO₂ content (<45 wt%). Only two samples (AV10A and AV10B) can be classified as alkaline in the abzarokite series.

In Figure 3, we also compare our results with ash and scoria deposit samples from the 2000–2001, 2010–2011, 2015–2016, and 2019 Bromo eruptions [23]. The results from their samples indicate a basaltic-andesite to basalt trachy-andesite melt source beneath the Bromo volcano, with a transition from a medium-K to a high-K composition (2010–2019) [23].



 $\label{eq:Figure 3. Classification of volcanic samples based on K_2O vs SiO_2 Data from Alfianti et al. [23] are plotted as references, while the boundary lines and corresponding rock classification are based on study [33].}$

Table 1. X-ray fluorescence (XRF) data of volcanic samples Bromo-Tengger-Semeru (BTS)

No.	Sample ID	Al ₂ O ₃	SiO ₂	K ₂ O	CaO	TiO ₂	V ₂ O ₅	Cr ₂ O ₃	MnO	Fe ₂ O ₃	CuO	SrO	BaO	Eu ₂ O ₃	Re ₂ O ₇	ZnO	P ₂ O ₅	Rb ₂ O
1	P1.1	12	44.8	3.87	11.8	2.14	0.06	0.051	0.35	23.2	0.11	0.33	0.2	0.29	0.2	0.01	0.83	0
2	P 1.2	12	46.5	4.26	11.3	2.04	0.05	0.047	0.29	21.3	0.099	0.3	0.23	0.33	0.2	0.006	0.89	0.11
3	P1.3	11	40.1	4.52	12.2	2.26	0.05	0.055	0.37	26.8	0.14	0.47	0.2	0.34	0.2	0.02	1	0
4	P 2.1	12	41.9	4.07	12.4	2.13	0.06	0.054	0.34	24.7	0.12	0.48	0.2	0.34	0.2	0.01	1.1	0
5	P 2.2	11	39.6	3.8	13.1	2.18	0.07	0.058	0.38	27.2	0.12	0.57	0.2	0.32	0.3	0.01	1.2	0.18
6	P 2.3	11	45.4	4.52	11.7	2.1	0.05	0.051	0.34	23.3	0.11	0.36	0.23	0.3	0.2	0.01	0	0
7	P2.4	0	48.7	5.04	13.3	2.38	0.05	0.058	0.4	28.2	0.14	0.44	0.26	0.38	0.2	0.01	0	0.18
8	P 2.7	12	45	4.18	12	2.13	0.05	0.047	0.34	22.8	0.11	0.35	0.2	0.31	0.2	0	0	0.11
9 10	P 2.8 P 3.1	12 13	43.1 46.5	4.27 4.1	12.6 12.4	2.11 1.85	0.04 0.04	0.047 0.045	0.35 0.31	24.2 21.2	0.12 0.11	0.4 0.35	0.2 0.2	0.29	0.2 0.2	0.01 0.01	0	0.13
11	P 4.1	12	44.8	4.02	12.4	2.02	0.04	0.043	0.31	22.3	0.11	0.33	0.2	0.3	0.2	0.01	0.99	0.12
12	P4.3	8.9	27.3	3.39	8	2.02	0.03	0.049	0.31	41.27	0.11	0.38	0.2	0.39	0.2	0.02	1.5	0.12
13	P 5.1	12	44.4	3.47	13.3	2.22	0.073	0.073	0.23	22.6	0.13	0.41	0.2	0.39	0.2	0.008	0	0
14	P 5.2	10	39.4	4.24	12.2	2.39	0.071	0.058	0.39	28.9	0.11	0.45	0.2	0.46	0.2	0.02	1	0
15	P 5.3	10	38.5	4.21	13.1	2.23	0.06	0.063	0.39	28.7	0.15	0.57	0.3	0.39	0.2	0.02	1.2	0
16	P 6.1	11	43.3	4.27	12.6	2.11	0.05	0.054	0.34	24.8	0.12	0.4	0.2	0.32	0	0	0	0
17	L2	9.4	38.6	3.04	11	3.28	0.1	0.051	0.39	31.9	0.14	0.3	0	0.45	0.2	0.03	0.93	0.14
18	L3	9.1	38	2.98	11.1	3.26	0.098	0.054	0.42	33	0.13	0.32	0	0.41	0.2	0.04	0.93	0
19	L4	9.1	37.3	2.92	10.9	3.17	0.083	0.061	0.44	34.2	0.14	0.4	0.2	0.4	0.3	0.03	0	0
20	L5	0	40.2	3.22	12.2	3.58	0.12	0.067	0.47	37.5	0.15	0.42	0	0.56	0.32	0.02	0.96	0.18
21	L6	9.3	38.3	2.91	11	3.08	0.086	0.062	0.42	32.3	0.14	0.37	0.2	0.37	0.2	0.03	1	0.15
22	L7	9.6	37.9	3	11	3.2	0.091	0.061	0.41	32.6	0.14	0.33	0	0.41	0.2	0.03	1	0
23	L8	9.1	38.5	2.68	10.7	3.25	0.11	0.063	0.42	34	0.15	0.33	0	0.42	0.2	0.03	0	0
24	L9	8.7	37.4	2.46	10.3	3.21	0.11	0.061	0.44	34.9	0.16	0.37	0	0.44	0.2	0.03	0.99	0.15
25	L10	8.5	36.3	2.71	10.8	3.18	0.11	0.056	0.77	35.1	0.17	0.44	0	0.48	0.2	0.04	1.2	0
26	AV1	8.9	36.7	3.28	11.4	3.09	0.088	0.061	0.45	33.4	0.13	0.38	0.2	0.43	0.27	0.02	1.2	0
27	AV2	8.7	37.5	3.34	11	3.14	0.08	0.057	0.46	33	0.14	0.38	0.2	0.41	0.2	0.04	1	0.17
28 29	AV3 AV4	9.2 9.8	38.9	3.44 3.4	11.6 10.8	3.08	0.087 0.085	0.055	0.44 0.41	31 30	0.13	0.36	0 0.2	0.4	0.2	0.03	1.2 0.9	0 0.15
30	AV5	9.8	40.1 40	2.93	10.6	3.01	0.083	0.047 0.054	0.41	31.67	0.13 0.14	0.35	0.2	0.36 0.38	0.2 0.2	0.03	0.9	0.13
31	AV6	9.8	37.7	2.68	11	3.14	0.078	0.059	0.42	33.8	0.14	0.41	0.2	0.38	0.2	0.04	0	0
32	AV7	11	41.9	3.11	10.8	2.9	0.092	0.054	0.38	29	0.10	0.29	0.2	0.32	0.2	0.03	0	0
33	AV8A	9.1	39	2.74	9.8	3.13	0.076	0.066	0.4	33.5	0.15	0.42	0	0.48	0.2	0.03	0.96	0
34	AV8B	9.3	39.7	2.98	10.5	3.02	0.076	0.062	0.41	31.5	0.13	0.38	0.2	0.41	0.2	0.03	1.1	0
35	AV9A1	0	39.7	3.48	11.1	3.33	0.08	0.066	0.53	38.7	0.23	0.5	0.2	0.48	0.2	0.05	1.2	0
36	AV9A2	9.3	39.7	3.44	10.1	2.98	0.06	0.055	0.41	31.3	0.14	0.38	0.2	0.39	0.2	0.05	1.1	0.16
37	AV9B	9.6	41.1	3.38	10.1	3.02	0.06	0.058	0.42	30.8	0.13	0.33	0.2	0.4	0.2	0.03	0	0
38	AV10A	0	45.3	3.54	11.6	3.29	0.09	0.059	0.46	34.3	0.12	0.37	0.2	0.42	0.3	0.03	0	0
39	AV10TA	11	43.6	3.28	9.19	2.8	0.075	0.055	0.36	28.1	0.11	0.31	0	0.36	0.2	0.03	1	0
40	AV10B	0	47	3.84	10.4	3.01	0.07	0.062	0.48	32.6	0.14	0.43	0.3	0.41	0.2	0.05	1.1	0
41	AV11	9.1	38.2	2.67	10.2	3.03	0.092	0.06	0.4	33.6	0.14	0.39	0.2	0.37	0.2	0.03	1	0.18
42	PS 1.1	15	42.6	1.39	16.3	1.77	0.097	0.05	0.34	21.4	0.085	0.29	0.07	0.31	0.17	0	0	0
43 44	PS 1.2 PS 1.3	15 15	43.8 44.1	1.49 1.52	16.2 16	1.57 1.57	0.068 0.072	0.057 0.048	0.37 0.37	20 20.1	0.078 0.079	0.37 0.35	0.1 0.1	0.26 0.25	0.2 0.18	0	0	0
44	PS 1.5	16	44.1	1.32	17.3	1.37	0.072	0.048	0.37	16.6	0.079	0.33	0.1	0.23	0.18	0	0	0
45	PS 1.3 PS 2.1	16	47.6	1.59	16.7	1.12	0.03	0.04	0.39	15.3	0.063	0.38	0.1	0.24	0.2	0	0	0
47	PS 2.2	16	48.5	1.49	16.4	1.19	0.05	0.045	0.29	14.7	0.084	0.32	0.09	0.22	0.17	0	0	0
48	PS 2.3	16	46.9	1.61	16.7	1.28	0.05	0.043	0.23	16.1	0.071	0.31	0.08	0.22	0.18	0	0	0
49	PS 2.4	17	46	1.4	19	1.18	0.057	0.038	0.27	14.2	0.066	0.35	0.07	0.24	0.17	0	ő	ő
50	PS 2.5	17	49.9	1.7	16.7	0.975	0.03	0.036	0.26	12.8	0.082	0.33	0.2	0.19	0.15	0	0	0
51	PS 3.1	16	31.4	0.37	13.7	2.17	0.13	0.076	0.54	34.02	0.14	0.37	0	0.41	0.27	0	0.81	0
52	PS 3.2	17	33.9	0.45	13.7	2.06	0.12	0.065	0.45	30.8	0.11	0.32	0	0.39	0.07	0.03	0.6	0
53	PS 3.3	16	34.2	0.45	15.3	2.08	0.14	0.069	0.43	30.8	0.11	0.31	0	0.39	0	0	0	0
54	PS 4.1	16	47.8	1.74	16.3	1.13	0.05	0.035	0.38	15.7	0.056	0.38	0.2	0.23	0.16	0	0	0
55	PS 4.2	16	45.4	2.42	15.3	1.2	0.03	0.043	0.43	17.9	0.083	0.47	0.2	0.28	0.2	0.007	0	0

Several researchers [24, 47] in the study of rock composition evolution have reported that the high-K affinity was considered to be induced by younger and post-caldera magma, while, in contrast, the medium-K rocks were attributed to pre-caldera. This means that all samples we took came from magma activities after the caldera in BTS was formed.

Basalt rocks with High-K can be estimated to have rare earth elements (REE) in the range of 90-610 ppm [48]. The REE ratios measured include La, estimated to have a ratio of 3.6-34 ppm, and Eu with a ratio of 0.24-0.40 ppm [49, 50]. This result can certainly be justified with further research so that the content of other critical minerals may also be mapped in the BTS area. Understanding the distribution and potential of REE in volcanic rock is crucial for resource exploration and environmental management.

Further classification uses the Si vs Fe ratio relation [34]. The Si vs Fe ratio is a key factor in the geochemical classification of sediments and minerals. It helps in distinguishing between different types of sediments and minerals based on their composition. Based on the results of geochemical tests carried out by volcanic samples in the BTS area, there is a lot of Fe, so the classification using this data is considered necessary to look at the type of rock based on the content of silica (Si) and iron (Fe) from the BTS volcanic sample.

The classification in Figure 4 shows that the BTS volcanic samples are aillikite. Aillikites are part of the broader group of ultramafic lamprophyres. In this case, these types of rocks have a small number of outcrops, especially those exposed on the surface. The classification results of the rocks at BTS, which are classified as ultramafic lamprophyre rock types, are apparently identical to the volcanic rocks in the Arjuno-Welirang Mountains [43]. Mount Arjuno-Welirang is located 75 km northwest of Mount Bromo. This suggests that these mountains had a similar tectonic setting during their formation.

Aillikites are enriched in REEs. Studies show that trace elements, especially REEs, show a general rise in levels from aillikites to other minerals, indicating their enrichment. Additionally, aillikites exhibit very REE-enriched patterns, particularly in LREEs (light rare earth elements) [51, 52].

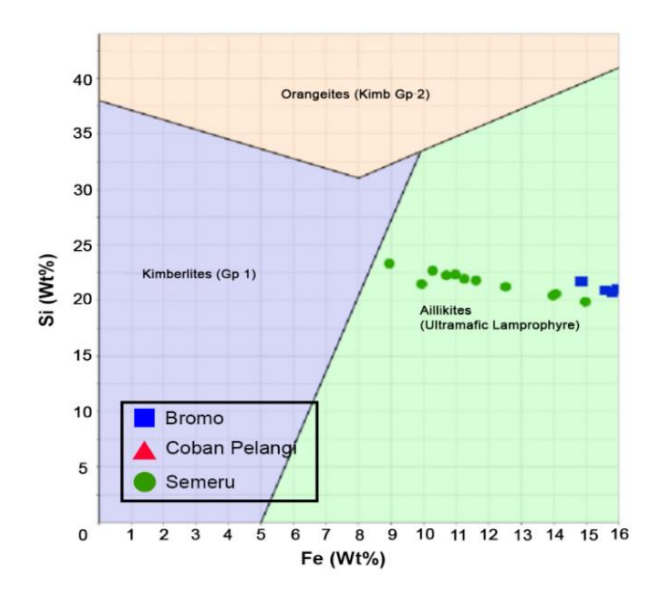


Figure 4. Classification of volcanic samples in the BTS area based on the Si vs Fe ratio

Boundary lines and corresponding rock classification are based on study [34].

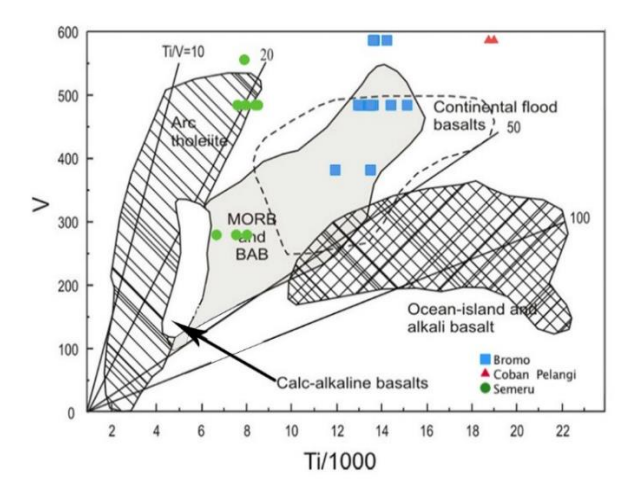


Figure 5. Ti-V diagram for basalts

The field of arc tholeites, MORB and back-arc basalts, continental flood basalts, ocean-island and alkali basalts are recognized by their Ti/V ratio, as shown in the study [35].

Based on the environment in which they are formed, volcanic materials can be classified according to several studies that have been conducted. Among the classifications carried out is research [35, 36]. Shervais [35] classifies volcanic rocks using the plot Ti vs. V. The Ti-V diagram is generally used for determining tectonic settings of mafic and ultramafic rocks, especially basalts, because it directly reflects mantle source characteristics and degree of partial melting. This Ti vs. V plot distinguishes the environment from which the rock comes from into four different arcs. Among the environments classified by the Ti vs V plot, namely, arc tholeiites, Mid Ocean Ridge Basalt (MORB), and Back-Arc Basalts (BAB), continental flood basalts, ocean-island, and alkali basalts (Figure 5).

Ultramafic rock are characterized by low TiO_2 contents (>2 wt%) and BTS volcanic samples (aillikite) have a range 1% - 3.58% TiO_2 (see Table 1) and a Ti/V ratio (Figure 5) showing a very large variation range from values roughly similar to those of typical arc tholeites (Ti/V <20 for some Semeru samples) to values between 20 to 50 for most samples. They are similar to typical MORB (or BAB) and continental flood basalts.

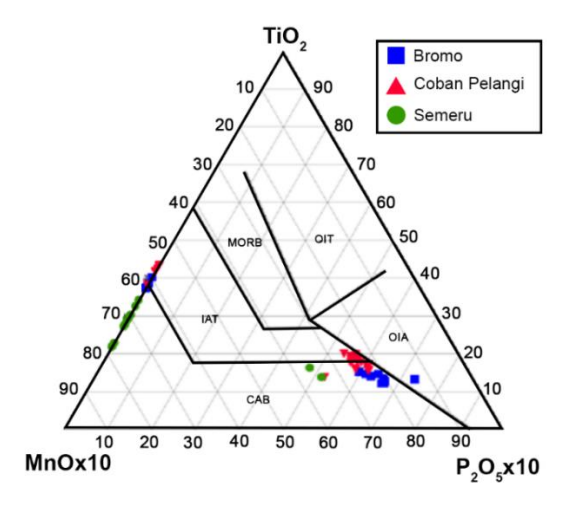


Figure 6. Ternary diagram of TiO₂-MnO×10-P₂O₅×10 for volcanic material in the BTS area Boundary lines and corresponding rock classification are based on study

[36].

To further study the magmatic evolution of the formation of volcanic samples in the BTS area, a ternary diagram analysis was carried out based on the comparison of the main elements MnO-TiO₂-P₂O₅ [36]. Based on the ternary diagram, the classification is divided into five different environments, including Mid-Ocean Ridge Basalt (MORB), Island Arc Tholeite (IAT), Calc-Alkaline Basalt (CAB), Seamount Tholeite (OIT), and Seamount Alkalic (OIA). Figure 6 shows that the volcanic material of the BTS area represents the most similarity with the Calc-Alkaline Basalt (CAB) and Island Arc Tholeite (IAT) environments.

The Calc-Alkaline Basalt (CAB) and Island Arc Tholeiite (IAT) magma series are the two most important igneous differentiation trends and are broadly expressed by the crustal dichotomy of andesitic continental crust and basaltic oceanic crust (MORB) [53]. Tholeiitic magmas may occur in all tectonic settings, while calc-alkaline magmas appear to be uniquely associated with the convergent margin setting [54], such as those at our study site. Furthermore, the Bromo-Tengger-Semeru (BTS) volcano indicates that the calcalkaline rocks would not be expected as a function of the depth of the Wadati-Benioff zone, whereas the Wadati-Benioff zone reaches a depth of about 100-150 km beneath the south coast of Java and approximately 600 km beneath the Java Sea [24].

4. CONCLUSION

Bromo-Tengger-Semeru (BTS) volcanic material geochemically contains natural compounds including Al₂O₃, SiO₂, K₂O, CaO, TiO₂, V₂O₅, Cr₂O₃, MnO, Fe₂O₃, CuO, SrO, BaO, Eu₂O₃, Re₂O₇, ZnO, P₂O₅, and Rb₂O. The dominant compounds from the geochemical test results include CaO (12.5 Wt%), Fe₂O₃ (27.5 Wt%), and SiO₂ (41.3 Wt%). The mapping carried out shows that SiO₂ content tends to be found in all areas of Bromo Semeru. Meanwhile, Fe₂O₃ is mostly found in outcrops in Coban Pelangi, and CaO is mostly found in the Semeru area. The dominance of Fe₂O₃ and differences in CaO and SiO₂ distribution in the BTS area reflect changes in magmatic processes or magmatic evolution as a product of volcanic activity in the research area.

Based on the K₂O vs SiO₂ classification, the rock types of the BTS volcanic material are mostly alkaline series absarokite, and some others are classified as high-K basalt types. The rocks with high K affinity are thought to be induced by the post-caldera stage, so it can be concluded that all samples originate from magma activity after the caldera at BTS was formed. Based on the Si vs Fe classification, BTS volcanic materials are classified in the ultramafic lamprophyre series as ailikites. The ailikite is thought to be enriched in REE, particularly in LREEs (light rare earth elements). They are also similar to typical MORB (or BAB) and continental flood basalts with a Ti/V ratio range of 20-50. Meanwhile, according to the classification of the main elements of MnO-TiO₂-P₂O₅, BTS volcanic materials represent the most similarity with the Calc-Alkaline Basalt (CAB) and Island Arc Tholeiite (IAT) environments. The CAB appears to be uniquely associated with the convergent margin setting; however, it is located in an area where talc-alkaline rocks would not be expected as a function of the depth of the Wadati-Benioff zone.

Finally, although this study provides information about the geochemical content of materials and infers their origin and mineralization potential at the study site, we also acknowledge the limitations of this study, especially in detailing the rare

earth elements (REE) content of high K basalt-type materials or rocks. Our focus in the future is on efforts to trace REE sources, determine their potential, predict REE volumes, and determine the priority scale of mining in a study area. Further exploration activities, such as Inductively Coupled Plasma Optical Emission Spectrometer (ICP-OES) measurements, are needed to confirm REE concentrations.

ACKNOWLEDGMENT

This work is supported by Institut Teknologi Sepuluh Nopember under the Capacity Development Program of Higher Education for Technology and Innovation Project Asian Development Bank Loan No 4110-INO, and Indonesian Collaborative Research (Contract 26/IT2/T/HK.00.01/V/2024), Universitas Negeri Malang (Contract number 5.4.38/UN32.14.1/LT/2024) and Universitas Negeri **Padang** (Contract number 219/UN35/KU/2024).

REFERENCES

- [1] Gan, J., Li, H., He, Z., Gan, Y., Mu, J., Liu, H., Wang, L. (2022). Application and significance of geological, geochemical, and geophysical methods in the Nanpo gold field in Laos. Minerals, 12(1): 96. https://doi.org/10.3390/min12010096
- [2] Ge, Y.Z., Zhang, Z.J., Cheng, Q.M., Wu, G.P. (2022). Geological mapping of basalt using stream sediment geochemical data: Case study of covered areas in Jining, Inner Mongolia, China. Journal of Geochemical Exploration, 232: 106888. https://doi.org/10.1016/j.gexplo.2021.106888
- [3] Pandarinath, K., García-Soto, A.Y., Santoyo, E., Guevara, M., Gonzalez-Partida, E. (2020). Mineralogical and geochemical changes due to hydrothermal alteration of the volcanic rocks at Acoculco geothermal system, Mexico. Geological Journal, 55(9): 6508-6526. https://doi.org/10.1002/gj.3817
- [4] Szemerédi, M., Lukács, R., Varga, A., Dunkl, I., Józsa, S., Tatu, M., Pál-Molnár, E., Szepesi, J., Guillong, M., Szakmány, G., Harangi, S. (2020). Permian felsic volcanic rocks in the Pannonian Basin (Hungary): New petrographic, geochemical, and geochronological results. International Journal of Earth Sciences, 109(1): 101-125. https://doi.org/10.1007/s00531-019-01791-x
- [5] Baldini, J.U.L., Lechleitner, F.A., Breitenbach, S.F.M., Van Hunen, J., Baldini, L.M., Wynn, P.M., Jamieson, R.A., Ridley, H.E., Baker, A.J., Walczak, I.W., Fohlmeister, J. (2021). Detecting and quantifying palaeoseasonality in stalagmites using geochemical and modelling approaches. Quaternary Science Reviews, 254: 106784.
 - https://doi.org/10.1016/j.quascirev.2020.106784
- [6] Mikheeva, E.A., Demonterova, E.I., Ivanov, A.V. (2021). Geochemistry of the Cheremkhovo and Lower Prisayan formations from the Jurassic Irkutsk Coal-Bearing Basin: Evidence for provenance and climate change in Pliensbachian—Toarcian. Minerals, 11(4): 357. https://doi.org/10.3390/min11040357
- [7] Edmonds, M. (2021). Geochemical monitoring of volcanoes and the mitigation of volcanic gas hazards. In

- Forecasting and Planning for Volcanic Hazards, Risks, and Disasters. Elsevier, pp. 117-151. https://doi.org/10.1016/B978-0-12-818082-2.00004-4
- [8] Martí, J. (2023). Volcano geology applications to ancient volcanism-influenced terrains: Paleovolcanism. In Updates in Volcanology - Linking Active Volcanism and the Geological Record. https://doi.org/10.5772/intechopen.108770
- [9] Doherty, M.E., Arndt, K., Chang, Z., Kelley, K., Lavin, O. (2023). Stream sediment geochemistry in mineral exploration: A review of fine-fraction, clay-fraction, bulk leach gold, heavy mineral concentrate and indicator mineral chemistry. Geochemistry: Exploration, Environment, Analysis, 23(4). https://doi.org/10.1144/geochem2022-039
- [10] Ghasemzadeh, S., Maghsoudi, A., Yousefi, M., Mihalasky, M.J. (2022). Information value-based geochemical anomaly modeling: A statistical index to generate enhanced geochemical signatures for mineral exploration targeting. Applied Geochemistry, 136: 105177.
 - https://doi.org/10.1016/j.apgeochem.2021.105177
- [11] Jabłońska, M., Rachwał, M., Wawer, M., Kądziołka-Gaweł, M., Teper, E., Krzykawski, T., Smołka-Danielowska, D. (2021). Mineralogical and chemical specificity of dusts originating from iron and non-ferrous metallurgy in the light of their magnetic susceptibility. Minerals, 11(2): 216. https://doi.org/10.3390/min11020216
- [12] Miwa, T., Ishibashi, H., Kazahaya, R., Okumura, S., Iguchi, M., Saito, G., Yasuda, A., Geshi, N., Kagi, H. (2023). Redox state of magma recorded in volcanic glass from an ash-forming eruption at Bromo volcano, Indonesia: Insights into the degassing process. Bulletin of Volcanology, 85(9): 48-62. https://doi.org/10.1007/s00445-023-01660-1
- [13] Clemens, J.D., Bryan, S.E., Stevens, G., Mayne, M.J., Petford, N. (2022). How are silicic volcanic and plutonic systems related? Part 2: Insights from phase-equilibria, thermodynamic modelling and textural evidence. Earth-Science Reviews, 235: 104250. https://doi.org/10.1016/j.earscirev.2022.104250
- [14] López-Saavedra, M., Martí, J. (2023). Reviewing the multi-hazard concept. Application to volcanic islands. Earth-Science Reviews, 236: 104286. https://doi.org/10.1016/j.earscirev.2022.104286
- [15] Boomeri, M., Naruyi, S., Ghodsi, M. (2020). Petrography and geochemistry of igneous rocks and Pb mineralization in Chasorbi area, south of Zahedan, southeastern Iran. Scientific Quarterly Journal of Geosciences, 29(116): 3-14. https://doi.org/10.22071/gsj.2019.135671.1490
- [16] Lerner, G.A., Piispa, E.J., Bowles, J.A., Ort, M.H. (2022). Paleomagnetism and rock magnetism as tools for volcanology. Bulletin of Volcanology, 84(3): 24-34. https://doi.org/10.1007/s00445-022-01529-9
- [17] Mariano, A.N., Mariano, A. (2012). Rare earth mining and exploration in North America. Elements, 8(5):369-376. https://doi.org/10.2113/gselements.8.5.369
- [18] Cochrane, J. (2006). Indonesian national parks: Understanding leisure users. Annals of Tourism Research, 33(4): 979-997. https://doi.org/10.1016/j.annals.2006.03.018
- [19] Bachri, S., Fathoni, M.N., Sumarmi, Masruroh, H., Wibowo, N.A., Khusna, N., Billah, E.N., Yudha, L.

- (2023). Geomorphological mapping and landform characterization of Semeru volcano after the eruption in 2021. IOP Conference Series: Earth and Environmental Science, 1180: 012004. https://doi.org/10.1088/1755-1315/1180/1/012004
- [20] Rochman, J.P.G.N., Buwonokeling, W.N., Fajar, M.H.M., Hilyah, A., Warnana, D.D., Lestari, W., Komara, E., Ariyanti, N., Azhali, F.M. (2024). Comparison of airborne magnetic and ground magnetic for identification of sub-surface condition study case sand caldera of Bromo-Tengger volcanic complex: Preliminary study. IOP Conference Series: Earth and Environmental Science, 1418: 012061. https://doi.org/10.1088/1755-1315/1418/1/012061
- [21] Wahyuningtyas, N., Yaniafari R.P., Rosyida, F., Megasari, R., Dewi, K., Khotimah, K. (2021). Mapping a eruption disaster-prone area in the Bromo-Tengger-Semeru National Tourism Strategic Area (Case study of Mount Semeru, Indonesia). GeoJournal of Tourism and Geosites, 39(4): 1430-1438. https://doi.org/10.30892/gtg.394sp114-787
- [22] Gunawan, R.M.P.P., Ikhwanushova, G., Harijoko, A., Wibowo, H.E., Setianto, A. (2021). Re-interpretation of distribution of Lautan Pasir caldera-forming eruption products, Bromo-Tengger Caldera Complex, East Java. IOP Conference Series: Earth and Environmental Science, 851: 012038. https://doi.org/10.1088/1755-1315/851/1/012038
- [23] Alfianti, H., Bani, P., Sumaryadi, M., Primulyana, S., Marlia, M., Saing, U.B., Haerani, N., Gunawan, H. (2022). Bromo activity over the last decade: Consistent passive degassing and source magma evolution. Geoscience Letters, 9: 15. https://doi.org/10.1186/s40562-022-00221-2
- [24] Van Gerven, M., Pichler, H. (1995). Some aspects of the volcanology and geochemistry of the Tengger Caldera, Java, Indonesia: Eruption of a K-rich tholeiitic series. Journal of Southeast Asian Earth Sciences, 11(2): 125-133. https://doi.org/10.1016/0743-9547(95)00003-B
- [25] Whitford, D.J., Nicholls, I.A., Taylor, S.R. (1979). Spatial variations in the geochemistry of Quaternary lavas across the Sunda arc in Java and Bali. Contributions to Mineralogy and Petrology, 70(3): 341-356. https://doi.org/10.1007/BF00375361
- [26] Siswowidjoyo, S., Sudarsono, U., Wirakusumah, A.D. (1997). The threat of hazards in the Semeru volcano region in East Java, Indonesia. Journal of Asian Earth Sciences, 15(2-3): 185-194. https://doi.org/10.1016/S0743-9547(97)00007-X
- [27] Thouret, J.C., Lavigne, F., Suwa, H., Sukatja, B. (2007). Volcanic hazards at Mount Semeru, East Java (Indonesia), with emphasis on lahars. Bulletin of Volcanology, 70: 221-244. https://doi.org/10.1007/s00445-007-0133-6
- [28] Thouret, J.C., Taillandier, M., Wavelet, E., Azzaoui, N., Santoni, O., Tjahjono, B. (2023). Semeru volcano, Indonesia: measuring hazard, exposure and response of densely populated neighbourhoods facing persistent volcanic threats. Natural Hazards, 117(2): 1405-1453. https://doi.org/10.1007/s11069-023-05910-5
- [29] Acquafredda, P. (2019). XRF technique. Physical Sciences Reviews, 4(8). https://doi.org/10.1515/psr-2018-0171
- [30] Martorelli, D. (2019). XRF/XRD combined

- spectroscopy for material characterization in the fields of Material science and Cultural heritage. Doctoral dissertation, University of Trento. https://doi.org/10.15168/11572 242657
- [31] Richards, M.J. (2019). Realising the potential of portable XRF for the geochemical classification of volcanic rock types. Journal of Archaeological Science, 105: 31-45. https://doi.org/10.1016/j.jas.2019.03.004
- [32] Sirbescu, M.L.C., Doran, K., Konieczka, V.A., Brennan, C.J., Kelly, N.M., Hill, T., Knapp, J., Student, J.J. (2023). Trace element geochemistry of spodumene megacrystals: A combined portable-XRF and micro-XRF study. Chemical Geology, 621: 121371. https://doi.org/10.1016/j.chemgeo.2023.121371
- [33] Peccerillo, A., Taylor, S.R. (1976) Geochemistry of eocene calc alkaline volcanic rocks from Kastamonu area, Northern Turkey. Contribution to Mineralogy and Petrology, 58: 63-81. https://doi.org/10.1007/BF00384745
- [34] Tappe, S., Foley, S.F., Jenner, G.A., Heaman, L.M., Kjarsgaard, B.A, Romer, R.L., Stracke, A., Joyce, N., Hoefs, J. (2006). Genesis of ultramafic lamprophyres and carbonatites at Aillik Bay, Labrador: A consequence of incipient lithospheric thinning beneath the North Atlantic Craton. Journal of Petrology, 47(7): 1261-1315. https://doi.org/10.1093/petrology/egl008
- [35] Shervais, J.W. (1982). Ti-V plots and the petrogenesis of modern and ophiolitic lavas. Earth and Planetary Science Letters, 59(1): 101-118. https://doi.org/10.1016/0012-821X(82)90120-0
- [36] Mullen, E.D. (1983). MnO/TiO₂/P₂O₅: A minor element discriminant for basaltic rocks of oceanic environments and its implications for petrogenesis. Earth and Planetary Science Letters, 62(1): 53-62. https://doi.org/10.1016/0012-821X(83)90070-5
- [37] Mulyadi, E. (1992). The Bromo-Tengger Complex (East Java, Indonesia). Structural and volcanological study. Doctoral dissertation, Clermont-Ferrand 2.
- [38] Santosa, S., Suwarti, T. (1992). Geological Map of Malang Sheet, Java. Geological Research an Development Centre, Republic of Indonesia. https://geologi.esdm.go.id/geomap/pages/preview/petageologi-lembar-kediri-jawa.
- [39] Suwarti, T. (1992). Geological map of the Probolinggo Quadrangle, Jawa. Geological Research and Development Centre. https://geologi.esdm.go.id/geomap//pages/preview/petageologi-lembar-malang-jawa.
- [40] Sujanto, Hadisantono, R., Kusnama, Chaniago, R., Baharuddin, R. (1992). Geological Map of the Turen Quadrangle, Jawa. Geological Research and Development Centre. https://geologi.esdm.go.id/geomap//pages/preview/petageologi-lembar-blitar-jawa.
- [41] Suwarti, T., Suharsono. (1992). Geological Map of the Lumajang Quadrangle, Jawa. Geological Research and Development Centre. https://geologi.esdm.go.id/geomap//pages/preview/petageologi-lembar-turen-jawa.
- [42] Johnson, D., Hooper, P., Conrey, R. (1999). XRF method XRF analysis of rocks and minerals for major and trace

- elements on a single low dilution Li-tetraborate fused bead. Advances in X-ray Analysis, 41: 843-867.
- [43] Zakly, H.'I., Zulaikah, S., Hapsoro, C.A., Maulida, S., Hasan, M.F.R. (2024). Chemical element analysis of Arjuno-Welirang igneous rocks. Environmental Science and Pollution Research. https://doi.org/10.1007/s11356-024-33495-4
- [44] Du, D.H., Tang, M., Li, W., Kay, S.M., Wang, X.L. (2022). What drives Fe depletion in calc-alkaline magma differentiation: Insights from Fe isotopes. Geology, 50(5): 552-556. https://doi.org/10.1130/G49705.1
- [45] Cao, Y., Wang, C.Y., Huang, F., Zhang, Z. (2018). Iron isotope systematics of the Panzhihua mafic layered intrusion associated with giant Fe-Ti oxide deposit in the Emeishan Large Igneous Province, SW China. Journal of Geophysical Research: Solid Earth, 124(1): 358-375. https://doi.org/10.1029/2018JB016466
- [46] Yang, J., Wang, C., Jin, Z., Jing, Z. (2025). Deep evolution of carbonated magmas controls ocean island basalt chemistry. Nature Communications, 16: 5276. https://doi.org/10.1038/s41467-025-60619-2
- [47] Santoso, N.A., Bijaksana, S., Kodama, K., Santoso, D., Dahrin, D. (2017). Multimethod approach to the study of recent volcanic ashes from Tengger Volcanic Complex, Eastern Java, Indonesia. Geosciences, 7(3): 63. https://doi.org/10.3390/geosciences7030063
- [48] Henderson, P. (1984). Chapter 1 General Geochemical Properties and Abundances of the rare earth elements. Developments in Geochemistry, 2: 1-32. https://doi.org/10.1016/B978-0-444-42148-7.50006-X
- [49] Tao, Y., Shen, L., Feng, C., Yang, R., Qu, J., Ju, H., Zhang, Y. (2022). Distribution of rare earth elements (REEs) and their roles in plant growth: A review. Environmental Pollution, 298: 118540. https://doi.org/10.1016/j.envpol.2021.118540
- [50] Zhang, L., Tao, C., Su, X., Lv, S., Zhou, J., Deng, X., Yu, C., Song, B. (2022). Characteristics of rare earth elements in the surface sediments of Southwest Indian Ridge: Implication of grain size for the identification of hydrothermal activity. Geo-Marine Letters, 42: 7. https://doi.org/10.1007/s00367-022-00729-8
- [51] Rock, N.M.S. (1986). The nature and origin of ultramafic lamprophyres: Alnöites and allied rocks. Journal of Petrology, 27(1): 155-196. https://doi.org/10.1093/petrology/27.1.155
- [52] Ashchepkov, I.V., Zhmodik, S.M., Belyanin, D.M., Kiseleva, O.N., Karmanov, N.S., Medvedev, N.S. (2024). Comparative mineralogy, geochemistry and petrology of the Beloziminsky Massif and its aillikite intrusions. Geosystems and Geoenvironment, 3(4): 100309. https://doi.org/10.1016/j.geogeo.2024.100309
- [53] Chin, E.J., Shimizu, K., Bybee, G.M., Erdman, M.E. (2018). On the development of the calc-alkaline and tholeitic magma series: A deep crustal cumulate perspective. Earth and Planetary Science Letters, 482: 277-287. https://doi.org/10.1016/j.epsl.2017.11.016
- [54] Miyashiro, A. (1974). Volcanic rock series in island arcs and active continental margins. American Journal of Science, 274: 321-355. https://doi.org/10.2475/ajs.274.4.321

Table A1. Bromo-Tengger Semeru (BTS) volcanic sample data

N-	Commis ID	UTM 2	Zone 49S	Committee Outside		
No.	Sample ID	Easting	Northing	Sample Origin	Sample Type	
1	P1.1	715753.03	9122552.17	Bromo	Volcanic Sand	
2	P 1.2	715753.03	9122552.17	Bromo	Volcanic Sand	
3	P1.3	715756.1	9122549.47	Bromo	Volcanic Sand	
4	P 2.1	715618.61	9122765.85	Bromo	Volcanic Sand	
5	P 2.2	715620.1	9122762.69	Bromo	Volcanic Sand	
6	P 2.3	715639.66	9122740.5	Bromo	Volcanic Sand	
7	P2.4	715679.31	9122683.01	Bromo	Volcanic Sand	
8	P 2.7	715696.53	9122710.03	Bromo	Volcanic Sand	
9	P 2.8	715623.57	9122802.09	Bromo	Volcanic Sand	
10	P 3.1	716610.82	9121968.2	Bromo	Volcanic Sand	
11	P 4.1	717215.49	9121974.32	Bromo	Volcanic Sand	
12	P4.3	717215.64	9121983.61	Bromo	Volcanic Sand	
13	P 5.1	717730.93	9121993.66	Bromo	Volcanic Sand	
14	P 5.2	717697.19	9122019.26	Bromo	Volcanic Sand Volcanic Sand	
15	P 5.3	717692.7	9122026.14	Bromo	Volcanic Sand Volcanic Sand	
16	P 6.1	717578.16	9121918.61	Bromo	Volcanic Sand Volcanic Sand	
17	L2	705581.53	9113976.58		Gravel	
18	L2 L3	705581.53	9113976.58	Coban Pelangi Coban Pelangi	Gravel	
19						
	L4	705581.53	9113976.58	Coban Pelangi	Gravel	
20	L5	705581.53	9113976.58	Coban Pelangi	Gravel	
21	L6	705581.53	9113976.58	Coban Pelangi	Gravel	
22	L7	705581.53	9113976.58	Coban Pelangi	Gravel	
23	L8	705581.53	9113976.58	Coban Pelangi	Gravel	
24	L9	705581.53	9113976.58	Coban Pelangi	Gravel	
25	L10	705581.53	9113976.58	Coban Pelangi	Gravel	
26	AV1	705581.53	9113976.58	Coban Pelangi	Volcanic Ash	
27	AV2	705581.53	9113976.58	Coban Pelangi	Volcanic Ash	
28	AV3	705581.53	9113976.58	Coban Pelangi	Volcanic Ash	
29	AV4	705581.53	9113976.58	Coban Pelangi	Volcanic Ash	
30	AV5	705581.53	9113976.58	Coban Pelangi	Volcanic Ash	
31	AV6	705581.53	9113976.58	Coban Pelangi	Volcanic Ash	
32	AV7	705581.53	9113976.58	Coban Pelangi	Volcanic Ash	
33	AV8A	705581.53	9113976.58	Coban Pelangi	Volcanic Ash	
34	AV8B	705581.53	9113976.58	Coban Pelangi	Volcanic Ash	
35	AV9A1	705581.53	9113976.58	Coban Pelangi	Volcanic Ash	
36	AV9A2	705581.53	9113976.58	Coban Pelangi	Volcanic Ash	
37	AV9B	705581.53	9113976.58	Coban Pelangi	Volcanic Ash	
38	AV10A	705581.53	9113976.58	Coban Pelangi	Volcanic Ash	
39	AV10TA	705581.53	9113976.58	Coban Pelangi	Volcanic Ash	
40	AV10B	705581.53	9113976.58	Coban Pelangi	Volcanic Ash	
41	AV11	705581.53	9113976.58	Coban Pelangi	Volcanic Ash	
42	PS 1.1	715071.86	9092007.6	Semeru	Volcanic Sand	
43	PS 1.2	715071.86	9092007.6	Semeru	Volcanic Sand	
44	PS 1.3	715071.86	9092007.6	Semeru	Volcanic Sand	
45	PS 1.5	715071.86	9092007.6	Semeru	Andesite	
46	PS 1.3 PS 2.1	720638.17	9092007.6	Semeru	Volcanic Sand	
	PS 2.1 PS 2.2					
47		720638.17	9096060.39	Semeru	Volcanic Sand	
48	PS 2.3	720638.17	9096060.39	Semeru	Volcanic Sand	
49	PS 2.4	720638.17	9096060.39	Semeru	Andesite	
50	PS 2.5	720638.17	9096060.39	Semeru	Sandy soils	
51	PS 3.1	724894.84	9108533.88	Semeru	Sandy soils	
52	PS 3.2	724894.84	9108533.88	Semeru	Sandy soils	
53	PS 3.3	724894.84	9108533.88	Semeru	Volcanic Sand	
54	PS 4.1	719160.06	9111497.43	Semeru	Andesite	
55	PS 4.2	719160.06	9111497.43	Semeru	Sandstone	